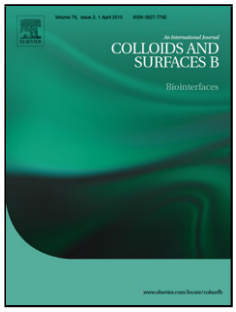

ANALYSIS OF THE STRUCTURE-FUNCTION RELATIONSHIP OF ALPHA AMYLASE COMPLEXED WITH POLYACRYLIC ACID

María C. Porfiri (Validation) (Formal analysis) (Conceptualization) (Methodology) (Writing - original draft) (Writing - review and editing) (Visualization), Natasha Melnichuk (Validation) (Formal analysis) (Methodology), Mauricio J. Braia (Validation) (Formal analysis) (Methodology), César Brinatti (Methodology) (Formal analysis) (Writing - original draft), Watson Loh (Investigation) (Supervision), Diana Romanini (Conceptualization) (Investigation) (Project administration)<ce:contributor-role>Writing - reviewing and editing) (Supervision) (Funding acquisition)

PII: S0927-7765(20)30017-5

DOI: https://doi.org/10.1016/j.colsurfb.2020.110787

Reference: COLSUB 110787

To appear in: *Colloids and Surfaces B: Biointerfaces*

Received Date: 30 September 2019

Revised Date: 30 December 2019

Accepted Date: 8 January 2020

Please cite this article as: Porfiri MC, Melnichuk N, Braia MJ, Brinatti C, Loh W, Romanini D, ANALYSIS OF THE STRUCTURE-FUNCTION RELATIONSHIP OF ALPHA AMYLASE COMPLEXED WITH POLYACRYLIC ACID, *Colloids and Surfaces B: Biointerfaces* (2020), doi: https://doi.org/10.1016/j.colsurfb.2020.110787

ANALYSIS OF THE STRUCTURE-FUNCTION RELATIONSHIP OF ALPHA AMYLASE COMPLEXED WITH POLYACRYLIC ACID

María C. Porfiri[a,d], Natasha Melnichuk[b,d], Mauricio J. Braia[b,d], César Brinatti[c], Watson Loh[c] and Diana Romanini[b,d*].

[a]Laboratorio de Investigación en Funcionalidad y Tecnología de Alimentos (LIFTA) - Departamento de Ciencia y Tecnología. Universidad Nacional de Quilmes (UNQ), Roque Sáenz Peña 352, Bernal, Buenos Aires, ARGENTINA.

[b]Instituto de Procesos Biotecnológicos y Químicos (IPROBYQ- CONICET). Facultad de Ciencias Bioquímicas y Farmacéuticas. Universidad Nacional de Rosario (UNR), Suipacha 531, Rosario, ARGENTINA.

[c]Instituto de Química, Universidade Estadual de Campinas (UNICAMP) Cidade Universitária Zeferino Vaz - Barão Geraldo, Campinas SP, BRAZIL.

[d]Consejo Nacional de Investigaciones Científicas y Técnicas (CONICET), Av. Rivadavia 1917 (C1033AAJ), Buenos Aires, Argentina

* send correspondence to:
Prof. Diana Romanini, Ph.D.
e-mail: dromanini@conicet.gov.ar; romanini@iprobyq-conicet.gob.ar
Instituto de Procesos Biotecnológicos y Químicos (IPROBYQ-CONICET)
Facultad de Ciencias Bioquímicas y Farmacéuticas
Universidad Nacional de Rosario.
ADDRESS Suipacha 531, (2000) Rosario, ARGENTINA
TELEPHONE NUMBER +54 341 480 4593 int 308
FAX +54 341 480 4598

Graphical abstract

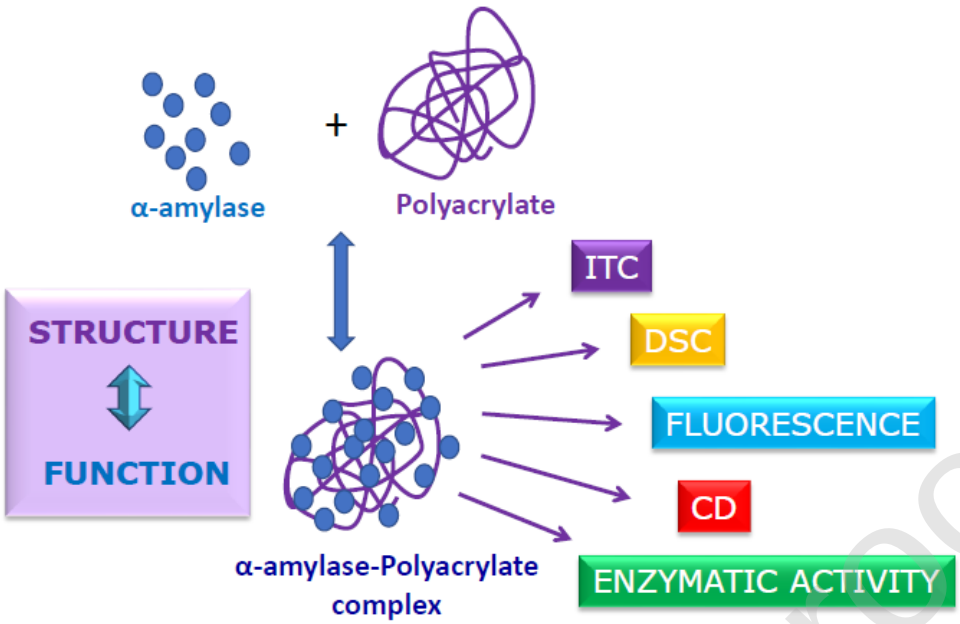

Highlights

- Amylase-polyacrylic acid interaction was addressed through several techniques
- Isothermal titration calorimetry revealed a mixed protein-polymer interaction
- Thermal unfolding process of amylase resulted partially reversible
- Amylase retains its catalytic activity in the polyacrylates presence

Abstract

Alpha-amylase is frequently used in technologies that require its immobilization, stabilization or encapsulation. Polyacrylic acid is a very suitable polymer for these purposes because it can bind to enzymes and then be released under certain conditions without altering the functional capacity of enzymes. The consequences produced by polyacrylic acid on alpha-amylase structure and function have been investigated through various techniques. Calorimetric measurements allowed examining the nature of the binding

reaction, stoichiometry and affinity, while spectroscopic techniques provided additional information about functional and structural perturbations of the enzyme. Isothermal titration calorimetry (ITC) revealed a mixed interaction and a binding model with a large number of molecules of protein per molecule of polyacrylic acid. One the one hand circular dichroism (CD) spectroscopy showed that alpha-amylase loses its secondary structure in the presence of increasing concentrations of polyacrylic acid, while it is stabilized by the polyelectrolyte at low pH. On the other hand, fluorescence spectra revealed that the three-dimensional enzyme structure was not affected in the microenvironment of tryptophan residues. Differential scanning calorimetry (DSC) thermograms showed that only one domain of alpha-amylase is affected in its conformational stability by the polymer. The unfolding process proved to be partially reversible. Finally, the enzyme retained more than 90% of its catalytic activity even in excess of the polymer.

Keywords: alpha-amylase; calorimetry; polyacrylic acid; spectroscopic analysis

1. Introduction

The formation of complexes between a polyelectrolyte (PEs) and protein is well known, and it is defined as the association between two polyions: one anionic and the other cationic. Therefore, these soluble/insoluble complex particles carry chemical groups which can be positively and negatively charged, and their components can be biomacromolecules or synthetic polymers [1,2]. For example, proteins interact strongly with both natural [3] and synthetic polymers, in particular with those carrying electrical net charges. They are commonly called smart polymers or polyelectrolytes [4–6].

As the degree of solvation decreases, protein-polyelectrolyte complexes can be soluble (strongly hydrated), coacervates (less hydrated) or, under conditions of large interaction, they can precipitate and generate a liquid-solid interface [7]. The precipitation of these complexes depends on different experimental parameters such as concentration, number and distribution of charged sites on the components, protein-polyelectrolyte ratio, pH and ionic strength of the medium, etc. [8–10].

Numerous studies are motivated by the applications of these complexes in the purification of proteins, control of protein release, enzyme immobilization and/or stabilization [7,11–15]. In a previous study, we have examined the parameters affecting the complex formation between alpha-amylase (α-Amy) from *Aspergillus oryzae* or 1, 4-α-D-Glucan glucanohydrolase, EC: 3.2.1.1 and the anionic polyelectrolyte called polyacrylic acid (PAA). We have determined at which pH stronger interactions occur, the stoichiometry, and salt dependence on the complex formation. We have also designed a method for the concentration and purification of alpha-amylase by precipitation with polyacrylate at different molecular weights [10].

Alpha-amylases are members of the same family (13) in the classification of glycoside hydrolase [16]. They are among the most important industrial enzymes and have great significance in present-day biotechnology. All the family members share a similar structure consisting of two main domains: I (C-terminus) and II (N-terminus). N-terminus domain is subdivided into two domains A and B. Domain A is a $(\beta/\alpha)_8$ - barrel, domain B is a loop between the β-3 strand and α-3 helix of domain A. Domain I is an extension at the C-terminus characterized by a “Greek key” conformation [17]. The enzyme is an endo-hydrolase that produces large oligosaccharides as products of starch degradation due to the

scission of internal α-1,4 linkages. It also has numerous applications, such as in the food and brewage industry and the production of biofuels [18–20].

Differential scanning calorimetry (DSC) is a universal method for studying the thermal denaturation of proteins. It does not rely on changes in the spectroscopic signal, as is the case with circular dichroism (CD), fluorescence and absorbance. Thereby, it has the advantage of measuring directly the heat absorption associated with the denaturation process, and it is more capable of resolving multiple overlapping processes [21].

A global analysis of polymer−protein interactions by different techniques can reveal the different possibilities of biotechnological applications.

The aims of this work were to determine the interaction nature between α-Amy and PAA at two different molecular weights (100,000 and 240,000 g/mol) and to analyze the structural and functional perturbation of the protein due to this interaction.

2. Materials and Methods

2.1. Chemicals:

α-Amy from *Aspergillus oryzae* was purchased from Sigma Chem. Co. (USA) and PAA, sodium salt, sol. in water, average molecular mass 240,000 g/mol, 25 wt. % (PAA 240,000) and 100,000 g/mol, 35 wt. % (PAA 100,000) were purchased from Aldrich and used without further purification. Phosphate buffer solutions pH 3.00 and 6.00 were prepared at a concentration of 50 mmol/L. They were adjusted with NaOH or HCl in each case.

2.2. ITC assays

Titrations were performed at 20 °C in a VP-ITC titration calorimeter (Northampton, MA, USA). 1.436 mL of α-Amy 22 g/L were first added to the sample cell. After baseline

stabilization, small aliquots ranging from 3 to 10 µL (0.31 and 0.58 %w/w for PAA 240,000 and 100,000, respectively) were added stepwise by an automatic syringe containing 270 µL of polymeric solution.

The reference cell contained Milli-Q grade water and all solutions were prepared in phosphate buffer 50 mM at pH 3.00 as the optimal interaction between α-Amy and PAA occurs at this pH [10].

The energy associated with the interaction between α-Amy and PAA was calculated by discounting the heat of protein and PAA dilution by the titration of buffer into protein solution and solution of PAA into the buffer, respectively. Data were fitted to a single set of identical and independent binding site model, where the total accumulative heat (Q) after N injections can be expressed as a function of the variables cell volume (Vc), total ligand concentration ($[L]_T$) and total macromolecule concentration ($[M]_T$) by the following equation [22],

$$Q = (Vc\Delta H^\circ / 2K)\left[1 + K[L]_T + nK[M]_T - \sqrt{(1 + K[L]_T + nK[M]_T)^2 - 4nK^2[M]_T[L]_T}\right] \quad (1)$$

By nonlinear regression of experimental data, the microscopic apparent constant of the binding equilibrium (*K*), the number of binding sites in the macromolecule for the ligand (*n*) and the enthalpic change per mol of bound ligand (ΔH°) were determined. The intrinsic molar free energy change (ΔG°) and the intrinsic molar entropy change (ΔS°) for the binding reaction were calculated by the fundamental thermodynamic equations 2 and 3,

$$\Delta G^\circ = -RT \ln K \quad (2)$$

$$\Delta S^\circ = \frac{(\Delta H^\circ - \Delta G^\circ)}{T} \quad (3)$$

The mathematical model equation selected to fit the ITC data (eq. 1) was derived by assuming that the macromolecule contains a single set of identical and independent sites

for binding, all with the same binding strength. In other words, the polyelectrolyte has *n independent and equivalent sites*, all of which have the same affinity constant, *K*, for the protein. It means that *n* moles of α-Amy are able to bind per mol of PAA. Titrations were also carried out in the presence of NaCl 1M in order to evaluate the effect of ionic strength on the interaction. The ΔH° of dilution of the protein and PAA in the buffer was subtracted.

2.3. CD Spectroscopy

CD spectra of α-Amy in the absence and in the presence of PAA were compared. Circular dichroism assays were carried out at a fixed protein concentration of 0.11 g/L and different concentrations of PAA. CD experiment must carry out at low absorbance medium to avoid the "inner filter effect"[23].

The stability of the secondary structure of α-Amy in the absence and in the presence of PAA was evaluated by obtaining the CD spectra at pH 6.00 after different periods of incubation at pH 3.00, at a fixed PAA:α-Amy ratio. Therefore, 2 mL of 5.5 g/L α-Amy solutions were prepared in phosphate buffer 50 mM at pH 3.00, by itself and in the presence of PAA. These solutions were incubated for five hours at 20 °C and the spectra were recorded at different times by diluting small aliquots in phosphate buffer at pH 6.00 until a concentration of α-Amy of 0.11 g/L was reached. These pH values were chosen because the enzyme is extremely stable at neutral pH (5.00 - 8.00) whereas it loses its activity below this range. Besides, pH 3.00 was suggested to be the pH of higher interaction between α-Amy and PAA [24].

Spectra were recorded from 200 to 260 nm in a Jasco J-810 Spectropolarimeter using a quartz cuvette (1 cm pathlength) at 20 °C, controlled by a Peltier system. The following

parameters were used: 50 nm min^{-1} scan speed, 1 mm bandwidth, 1 s response and 7 accumulations. Spectra were corrected for the baseline contribution of the buffer.

2.4. Fluorescence Spectroscopy

Measurements were carried out in an Aminco-Bowman Serie 2-Fluorospectrometer with a 1 cm pathlength quartz cuvette, at 20 °C. The parameters used were: 100 nm min^{-1} scan speed, 4 nm bandwidth and 3 repetitive cycles. An excitation wavelength of 280 nm was applied while emission spectra were recorded in the range between 300 to 450 nm. Solutions were prepared in phosphate buffer 50 mM at pH 3.00 and all fluorescence spectra were corrected by the baseline contribution of the buffer. Intrinsic florescence was measured at different polymer:protein ratios, PAA 240,000: α-Amy ratios: 1:135; 1:126; 1:117; 1:88, PAA 100,000: PAA: α-Amy ratios: 1:46, 1:42, 1:39, 1:25, and α-Amy alone (0.55 g/L).

2.5. DSC assays

Thermal denaturation of α-Amy in the absence and in the presence of PAA was performed with a high sensitivity differential scanning calorimeter VP-DSC, MicroCal Inc.[25]. Solutions of α- Amy 22 g/L were prepared in phosphate buffer 50 mM, pH 6.00; in the absence and in the presence of the polymer (PAA:α-Amy molar ratio 1:154 and 1:52 for PAA 240,000 and 100,000, respectively). The scanning was performed in triplicate, between 35-85 °C at a scan rate of 0.5 °C min^{-1} and a constant pressure of 193 kPa. Buffer baseline scans were determined by 10 repetitions and subtracted from α-Amy transition scans prior to normalization and analysis of the denaturation of α-Amy. These calorimetric data were

analyzed using the software MicroCal Inc. ORIGIN 7.0, according to the methodology recommended by IUPAC. The parameters obtained from this analysis were: the temperature at which maximum heat exchange occurs (*Tm*) and the area under the peak which represents the enthalpy of transition (ΔH_{cal}) [26]. In order to check reversibility of α-Amy thermal denaturation, a first scanning and reheating (second scanning) of the sample were assayed under identical conditions.

The *Two-State Irreversible Model* (Eq. 5) is a limiting case for the Lumry and Eyring non-equilibria model [27], which suggests that the denaturation process of proteins is given by (Eq. 4):

$$N \xrightarrow{k} F \qquad (4)$$

where N is the native state, F is a final state (irreversibly denatured) of the protein originated by irreversible alterations, and k the velocity constant. The activation energy ($E^{\#}$) and the T at k=1 min^{-1} (T*) were determined according to the Two-State Irreversible Model by applying the four validation methods reported in literature [28–30].

The effect of α-Amy concentration was analyzed at 5.5, 22, 41.25 and 55 g/L, phosphate buffer pH 6.00 and 3.00, 50mM in the presence and in the absence of PAA at a scan rate of 0.5 °C min^{-1}. The effect of scan rate was evaluated at 0.25, 0.5, 1.0 and 1.5 °C min^{-1}, at α-Amy concentration of 22 g/L in the same medium conditions.

2.6. Enzymatic activity assays

α-Amy activity was determined with a commercial kit Amylase 405, kinetic-Unitest from Wiener Lab, Rosario, Argentina. α-Amy hydrolyzes the specific substrate 2-chloro-p-nitrophenyl-α-D-maltotriose (CNP-G3). The reaction was followed by measuring the

absorbance of the released reaction product, 2-chloro-p-nitrophenol (CNP), which absorbs at 405 nm (ε_{405} = 12.9 mM^{-1} cm^{-1}), for 5 min. The activity was calculated from the slope of the linear part of the graph of absorbance vs. time [20] and expressed in unit "U". One unit of enzyme activity was defined as the amount of enzyme required to hydrolyze 1 µmol of substrate per minute. The enzyme assays were performed at a constant temperature of 20 °C in the presence and in the absence of PAA. PAA:α-Amy molar ratios were chosen from the ITC results, 1:137 (PAA 100,000) and 1:476 (PAA 240,000), in phosphate buffer solutions 50mM, pH 6.00.

2.7. Statistical Analysis

Experiments were done in triplicate and reported results represent the mean from three calculated values and their standard deviations. Statistical analysis of the results was carried out using SigmaPlot SPW11.

3. Results and Discussion

3.1. Characterization of PAA/α-Amy binding by ITC

Figure 1 shows the heat of interaction between protein and PAA. Nonlinear fittings of experimental data are also shown in this figure. The heats associated to protein and PAA dilution were much smaller than PAA/α-Amy interaction (data not shown), and they were subtracted in Figure 1. Table 1 shows the thermodynamic parameters for the protein-polymer binding.

According to Section 2.2, *n* was defined as the number of *independent and equivalent sites* in PAA for α-Amy binding. As it was expected, *n* values (Table 1) were smaller than one, which indicates that several α-Amy molecules bind per molecule of PAA, *n* = 476 and 137,

for PAA 240,000 and 100,000, respectively. This indicates that the longer the polymer, the higher the number of α-Amy molecules are able to bind per PAA molecule, suggesting a higher precipitation power for PAA 240,000 than 100,000. The same conclusions were previously obtained by turbidimetric techniques [10].

The binding constant, *K*, was higher for PAA 240,000 than PAA 100,000, indicating a higher affinity between α-Amy and PAA 240,000 in comparison with PAA 100,000. Both cases showed negative ΔH°, indicating an exothermic interaction regardless the polymer length, due to electrostatic interaction between the protein and the polymer. A positive ΔS° value can be related to hydrophobic interactions between α-Amy and PAA. Although the complex formation would seem to lead to a decrease in entropy, the huge increase in degrees of freedom from the water molecules released to the bulk of the solution may be the main factor contributing to the ΔS° signal. Also, possibly the loss of structure in α-Amy would contribute to generate disorder. This combination of enthalpic and entropic effects suggests that the complex formation between α-Amy and PAA is both enthalpically and entropically driven, since both factors (ΔH° and ΔS°) contribute to a negative value of the total Gibbs energy (ΔG°).

The effect of ionic strength on complex formation is also shown in Figure 1 and the binding parameters in Table 1. For both PAA 240,000 and 100,000, the interaction is predominantly exothermic, which demonstrates that the presence of NaCl 1M does not hinder completely the electrostatic interactions between α-Amy and PAA. The number of α-Amy molecules bound per molecule of PAA (*n*) were: 313 ± 3 and 76 ± 1 for PAA 240,000 and 100,000, respectively. These values were smaller than those obtained in the absence of NaCl, which indicates that an increase in the ionic strength of the medium reduces the number of proteins bound per molecule of PAA. The other thermodynamic parameters shown in Table

1 related to the strength of the interaction were not significantly affected by the presence of NaCl 1M. These results confirm that the increase of the ionic strength of the medium was not suitable for the total dissociation of the complexes [10].

3.2. Conformational stability of α*-Amy secondary structure in the presence of PAA.*

Figure 2 shows the CD spectra of α-Amy in the absence and in the presence of different concentrations of PAA. The PAA:α-Amy ratios correspond to values close to complex stoichiometries and in excess of PAA [10] . In all spectra, two negative peaks appeared around 222 and 208 nm. However, the band at 222 nm has a higher intensity than the band at 208 nm, which indicates the presence of α/β domains in protein [17], in accordance with the conformational structure of α-Amy previously explained (Section 1). In addition, CD intensities were smaller as the concentration of PAA increases, which suggests that the secondary structure of α-Amy is more extensively broken at higher concentrations of PAA. Figure S-1 shows the CD spectra recorded for α-Amy at different periods of incubation at pH 3.00, in the absence and the presence of PAA. PAA:α-Amy ratios correspond to a complex stoichiometry for each case reported in a previous work [10] . While the initial spectrum of α-Amy alone exhibited the two characteristic peaks for α-Amy at around 222 and 208 nm, at 2.3 h and 5 h of incubation a major negative peak at 200 nm was observed. This indicates changes in the secondary structure of the protein, mainly the appearance of unordered segments, as the enzyme is incubated in acidic medium. A similar behavior was observed for α-Amy in the presence of PAA (Figure S-1B and C), and a considerable loss of secondary structure was observed during incubation. Although less intense, the peaks at 222 nm and 208 nm remain. . This indicates that the loss of secondary structure elements of α-Amy is delayed in the presence of PAA. These results suggest a stabilizing effect of the

polyelectrolytes on the structure of the enzyme, pronounced for the PAA with higher molecular weight.

3.3. Effects of PAA on enzymatic activity of α*-Amy.*

Several investigations have reported that polymers stabilize a variety of enzymes. It has been suggested that electrostatic interactions between enzymes and polyelectrolytes play a primary role, both in catalytic activity and conformational stabilization [12,31]. Figure 3 shows the enzymatic activity of α-Amy in the absence and in the presence of PAA. In spite of the changes in the secondary structure, previously suggested by CD spectra (Section 3.2), the enzymatic activity of α-Amy did not change significantly in the presence of PAA. These results suggest that the polymer-protein interaction does not affect the active site conformation of α-Amy.

3.4. Fluorescence spectroscopy of α*-Amy in the absence and in the presence of PAA.*

Fluorescence spectroscopy is a powerful technique to monitor the unfolding process and conformational changes in proteins. In this study, we examined two aspects of the fluorescence emission spectra of α-Amy in the presence of PAA: a) the intensity of the emitted fluorescence light, which can vary significantly due to dynamic or static quenching phenomena; b) the maximum wavelength (λ_{max}) shift, which depends on changes in the microenvironment of the tryptophan chromophore [32].

Figure 4 shows the fluorescence spectra obtained for α-Amy in the absence and in the presence of different concentrations of PAA. The PAA:α-Amy ratios correspond to values close to complex stoichiometries and in excess of PAA [10]. The spectra exhibited λ_{max} around 334 nm, which corresponds to the emission wavelength of tryptophan residues that

are located in the interior of the protein structure (superficial tryptophans have a much more polar environment, and so their λ_{max} are red shifted) [33]. Both figures (4A and 4B) show that the intensity of emitted light (FI) decreases as the concentration of PAA increases, possibly due to quenching phenomena. Furthermore, the presence of PAA did not vary significantly the λ_{max} position of α-Amy, which indicates that the three-dimensional structure of the enzyme in the microenvironment of the tryptophans is not significantly affected. It is worth noting that in other studies a red shift in λ_{max} in the fluorescence emission spectra was attributed to unfolded states [33].

3.5. *The effect of PAA on the thermal denaturalization of* α*-Amy.*

Figure 5 shows the thermal unfolding of α-Amy in the absence and in the presence of PAA 240,000 and 100,000, and Table 2 shows the parameters from the deconvolution of both curves. α-Amy presented two transitions, which indicates that the two domains of the enzyme independently unfold from one another. Moreover, the shape and intensity of the α-Amy melting peak were modified in the presence of PAA. According to the parameters in Table 2, in the presence of PAA (240,000 and 100,000) the Tm of the first transition (Tm_1) was slightly shifted to lower temperature values, while the values of $\Delta H_{cal\ 1}$ increased. This indicates that PAA strongly interacts with the first α-Amy domain, and alters its unfolding mechanism. The Tm of the second transition (Tm_2) remained constant, but their $\Delta H_{cal\ 2}$ values increased. This suggests that PAA do not affect significantly the conformational stability of the second α-Amy domain.

Although both polymers have the same monomeric unit, their behavior in solution is different due to their different molecular weight. This affects their solubility, gyration radius, hydration, viscosity, etc. The interaction between PAA/α-Amy is a complex process,

since both molecules have hydrophobic regions and net charges that vary according to the pH of the solution. Values of ΔH_{cal} (Table 2) for PAA 100,000 were larger than for PAA 240,000. This suggests that both PAA presents different interactions with α-Amy, probably due to different forces involved and the conformations adopted by polymers in the solution. The analysis of the thermal unfolding reversibility (second scanning) suggests that the first domain in α-Amy was severely affected by the thermal unfolding, in comparison with the second domain, mainly in the presence of PAA. In fact, almost no thermal effects were observed during the second heating cycle for the first domain in the presence of PAA 240,000 and 100,000 (Table 2). Besides, Tm_1 changed as the scan rate increases (Figure 6), but this was not observed for Tm_2 (data not shown). Both the changes in the thermogram in the second scanning and the dependence of Tm on the scan rate indicate that the thermal denaturation of α-Amy involves an irreversible process. This means that the process is kinetically controlled [27].

The influence of the α-Amy concentration in the absence and in the presence of PAA on the thermograms was assayed by measuring Tm vs. α-Amy concentration (data not shown). No changes were observed in Tm values, which suggest that thermal denaturation does not induce oligomerization.

Table 2 shows the kinetic parameters ($E^{\#}$ and T*) determined according to the *two-state irreversible model* for the first transition of α-Amy unfolding process. $E^{\#}$ and T* values did not change in the absence and presence of PAA. We can conclude that the presence of PAA does not alter the kinetics of thermal denaturation of α-Amy.

4. Conclusions

Although the interaction between proteins and polyelectrolytes has been widely studied, the structural and functional consequences of the interaction between α-Amy and PAA have not been studied in depth. This work provides a thorough understanding of the forces that are involved in the formation of polyelectrolyte-protein complexes and the factors that could put in risk the enzyme stability. These results have demonstrated that only one domain of α-Amy interacts strongly with PAA, and that a large number of enzyme molecules bind to one molecule of the polyelectrolyte with high affinity. Despite *Borisov et al* described the interaction between proteins and polyelectrolytes as a charged relationship, in this work we conclude that this interaction are both hydrophobic and electrostatically driven [34].

Finally, the results showed that the polymer could be useful for biotechnological applications where the enzyme must be immobilized, encapsulated, have its release controlled or precipitated without affecting its catalytic capability.

Acknowledgments

We would like to thank the staff from the English Department (FCByF-UNR) for the language correction of the manuscript. This work was supported by a grant from Agencia Nacional de Promoción Científica y Tecnológica (PICT 2013-1730; PICT 2016-1170), and CONICET (PIP 2015-505; PUE BD 2016 0041CO), Argentina.

REFERENCES

[1] A.B. Kayitmazer, D. Seeman, B.B. Minsky, P.L. Dubin, Soft Matter, 11 (2013) 2553–2583. doi:10.1039/c2sm27002a.

[2] W.S. Kim, I. Hirasawa, W.S. Kim, Effects of experimental conditions on the mechanism of particle aggregation in protein precipitation by polyelectrolytes with a high molecular weight, Chem. Eng. Sci. 56 (2001) 6525–6534. doi:10.1016/S0009-2509(01)00311-6.

[3] A. Lali, A. N., R. John, D. Thakrar, Reversible precipitation of proteins on carboxymethyl cellulose, Process Biochem. (2000). doi:10.1016/S0032-9592(99)00138-7.

[4] H. Priya James, R. John, A. Alex, K.R. Anoop, Smart polymers for the controlled delivery of drugs – a concise overview, Acta Pharm. Sin. B. 4 (2014) 120–127. doi:10.1016/j.apsb.2014.02.005.

[5] S. Anandhakumar, V. Nagaraja, A.M. Raichur, Reversible polyelectrolyte capsules as carriers for protein delivery, Colloids Surfaces B Biointerfaces. 78 (2010) 266–274. doi:10.1016/j.colsurfb.2010.03.016.

[6] S. Wang, K. Chen, A.B. Kayitmazer, L. Li, X. Guo, Tunable adsorption of bovine serum albumin by annealed cationic spherical polyelectrolyte brushes, Colloids Surfaces B Biointerfaces. 107 (2013) 251–256. doi:10.1016/j.colsurfb.2013.02.026.

[7] C.L. Cooper, P.L. Dubin, A.B. Kayitmazer, S. Turksen, Polyelectrolyte-protein complexes, Curr. Opin. Colloid Interface Sci. 10 (2005) 52–78. doi:10.1016/j.cocis.2005.05.007.

[8] M.J. Braia, D.B. Loureiro, G. Tubio, D. Romanini, Characterization of the Interaction

Between Pancreatic Trypsin and an Enteric Copolymer as a Tool for Several Biotechnological Applications, Colloids Surfaces B Biointerfaces. 136 (2015). doi:10.1016/j.colsurfb.2015.10.037.

[9] W. Kim, I. Hirasawa, W. Kim, E ects of experimental conditions on the mechanism of particle aggregation in protein precipitation by polyelectrolytes with a high molecular weight, 56 (2001) 6525–6534.

[10] M.C. Porfiri, G. Picó, B. Farruggia, D. Romanini, Insoluble complex formation between alpha-amylase from Aspergillus oryzae and polyacrylic acid of different molecular weight, Process Biochem. 45 (2010). doi:10.1016/j.procbio.2010.07.006.

[11] Z. Qu, F. Hu, K. Chen, Z. Duan, H. Gu, H. Xu, A facile route to the synthesis of spherical poly(acrylic acid) brushes via RAFT polymerization for high-capacity protein immobilization, J. Colloid Interface Sci. 398 (2013) 82–87. doi:10.1016/j.jcis.2013.02.001.

[12] F. Hilbrig, R. Freitag, P rotein purification by affinity precipitation, 790 (2003) 79–90. doi:10.1016/S1570-0232(03)00081-3.

[13] D. Djabali, N. Belhaneche, B. Nadjemi, V. Dulong, L. Picton, Relationship between potato starch isolation methods and kinetic parameters of hydrolysis by free and immobilised α-amylase on alginate (from Laminaria digitata algae), J. Food Compos. Anal. (2009). doi:10.1016/j.jfca.2008.11.001.

[14] K. Letchford, H. Burt, A review of the formation and classification of amphiphilic block copolymer nanoparticulate structures: micelles, nanospheres, nanocapsules and polymersomes, Eur. J. Pharm. Biopharm. 65 (2007) 259–269. doi:10.1016/j.ejpb.2006.11.009.

[15] M. Mohammadi, M. Khakbaz Heshmati, K. Sarabandi, M. Fathi, L.T. Lim, H.

Hamishehkar, Activated alginate-montmorillonite beads as an efficient carrier for pectinase immobilization, Int. J. Biol. Macromol. 137 (2019) 253–260. doi:10.1016/j.ijbiomac.2019.06.236.

[16] K.K. Ghadikolaei, M. Shojaei, A. Ghaderi, F. Hojjati, K.A. Noghabi, H.S. Zahiri, Biochemical properties of Glu-SH3 as a family 13 glycoside hydrolase with remarkable substrate specificity for trehalose: Implications to sequence-based classification of CAZymes, Arch. Biochem. Biophys. (2016). doi:10.1016/j.abb.2016.05.007.

[17] T. Bhanja Dey, R. Banerjee, Purification, biochemical characterization and application of α-amylase produced by Aspergillus oryzae IFO-30103, Biocatal. Agric. Biotechnol. 4 (2015) 83–90. doi:10.1016/j.bcab.2014.10.002.

[18] M.S. Hernández, M.R. Rodríguez, N.P. Guerra, R.P. Rosés, Amylase production by Aspergillus niger in submerged cultivation on two wastes from food industries, J. Food Eng. 73 (2006) 93–100. doi:10.1016/j.jfoodeng.2005.01.009.

[19] Z. Kádár, A.D. Christensen, M.H. Thomsen, A.B. Bjerre, Bioethanol production by inherent enzymes from rye and wheat with addition of organic farming cheese whey, Fuel. 90 (2011) 3323–3329. doi:10.1016/j.fuel.2011.05.023.

[20] G. Muralikrishna, M. Nirmala, Cereal α-amylases—an overview, Carbohydr. Polym. 60 (2005) 163–173. doi:10.1016/j.carbpol.2004.12.002.

[21] S.O. Hashim, R.-H. Kaul, M. Andersson, F.J. Mulaa, B. Mattiasson, Differential scanning calorimetric studies of a Bacillus halodurans alpha-amylase., Biochim. Biophys. Acta. 1723 (2005) 184–191. doi:10.1016/j.bbagen.2005.03.004.

[22] W. Kim, Y. Yamasaki, K. Kataoka, Development of a fitting model suitable for the isothermal titration calorimetric curve of DNA with cationic ligands, J. Phys. Chem. B. 110 (2006) 10919–10925.

[23] D.E. Epps, T.J. Raub, V. Caiolfa, A. Chiari, Determination of the Af ® nity of Drugs toward Serum Albumin by Measurement of the Quenching of the Intrinsic Tryptophan Fluorescence of the Protein, (1999) 41–48.

[24] M. Carlsen, J. Nielsen, J. Villadsen, Kinetic studies of acid-inactivation of α-amylase from Aspergillus oryzae, Chem. Eng. Sci. 51 (1996) 37–43. doi:10.1016/0009-2509(95)00233-2.

[25] P. Raviyan, J. Tang, B.A. Rasco, Thermal stability of α-amylase from Aspergillus oryzae entrapped in polyacrylamide gel, J. Agric. Food Chem. 51 (2003) 5462–5466. doi:10.1021/jf020906j.

[26] N.C. Garbett, G.N. Brock, Differential scanning calorimetry as a complementary diagnostic tool for the evaluation of biological samples, Biochim. Biophys. Acta - Gen. Subj. 1860 (2016) 981–989. doi:10.1016/j.bbagen.2015.10.004.

[27] J.M. Sanchez-Ruiz, Theoretical analysis of Lumry-Eyring models in differential scanning calorimetry., Biophys. J. 61 (1992) 921–935.

[28] M. Amani, A. a. Moosavi-Movahedi, G. Floris, A. Mura, B.I. Kurganov, F. Ahmad, A. a. Saboury, Two-state irreversible thermal denaturation of Euphorbia characias latex amine oxidase, Biophys. Chem. 125 (2007) 254–259. doi:10.1016/j.bpc.2006.08.006.

[29] G. Žoldák, E. Sedlák, E. Valušová, A. Wolfrum, J. Marek, M. Antalík, M. Sprinzl, Irreversible thermal denaturation of elongation factor Ts from Thermus thermophilus effect of the residual structure and intermonomer disulfide bond, Biochim. Biophys. Acta - Proteins Proteomics. 1764 (2006) 1277–1285. doi:10.1016/j.bbapap.2006.04.011.

[30] L.S. Zamorano, D.G. Pina, F. Gavilanes, M.G. Roig, I.Y. Sakharov, A.P. Jadan, R.B. Van Huystee, E. Villar, V.L. Shnyrov, Two-state irreversible thermal denaturation of anionic

peanut (Arachis hypogaea L.) peroxidase, Thermochim. Acta. 417 (2004) 67–73. doi:10.1016/j.tca.2004.01.018.

[31] M.C. Porfiri, B.M. Farruggia, D. Romanini, Bioseparation of alpha-amylase by forming insoluble complexes with polyacrylate from a culture of Aspergillus oryzae grown in agricultural wastes, Sep. Purif. Technol. 92 (2012). doi:10.1016/j.seppur.2012.03.004.

[32] J.R. Lakowicz, Principles of fluorescence spectroscopy, 2006. doi:10.1007/978-0-387-46312-4.

[33] C. Duy, J. Fitter, How aggregation and conformational scrambling of unfolded states govern fluorescence emission spectra, Biophys. J. 90 (2006) 3704–3711. doi:10.1529/biophysj.105.078980.

[34] A.L. Becker, K. Henzler, N. Welsch, M. Ballauff, O. Borisov, Proteins and polyelectrolytes: A charged relationship, Curr. Opin. Colloid Interface Sci. 17 (2012) 90–96. doi:10.1016/j.cocis.2011.10.001.

FIGURES

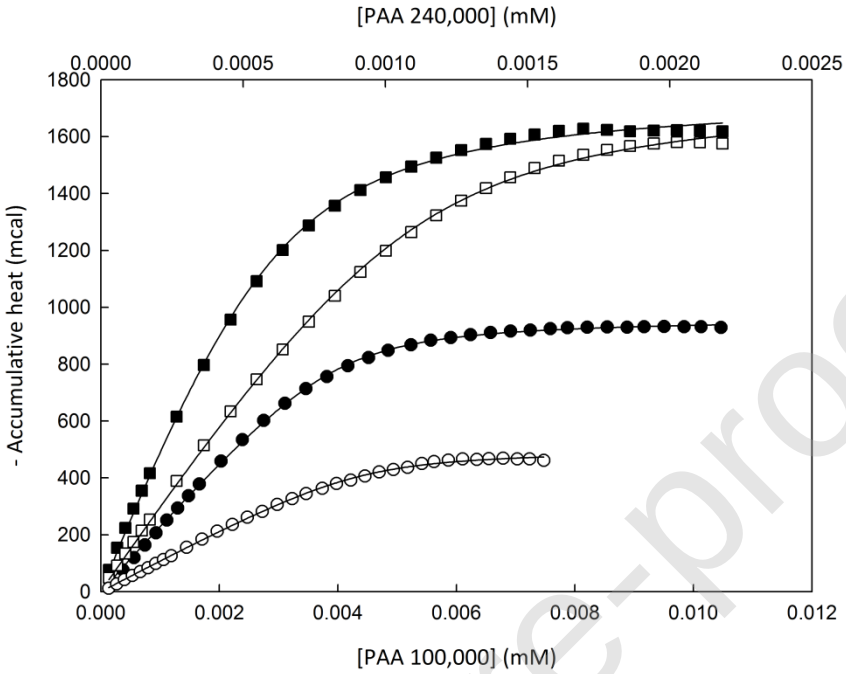

Figure 1: Binding curve for the calorimetric titration of 22 g/L α-Amy into PAA at 20°C. Accumulative heat vs [PAA] in the absence of NaCl: (●) PAA 240,000 and (■) PAA 100,000; and in the presence of NaCl 1 M: (○) PAA 240,000 and (□) PAA 100,000. Medium phosphate buffer 50 mM, pH 3.00.

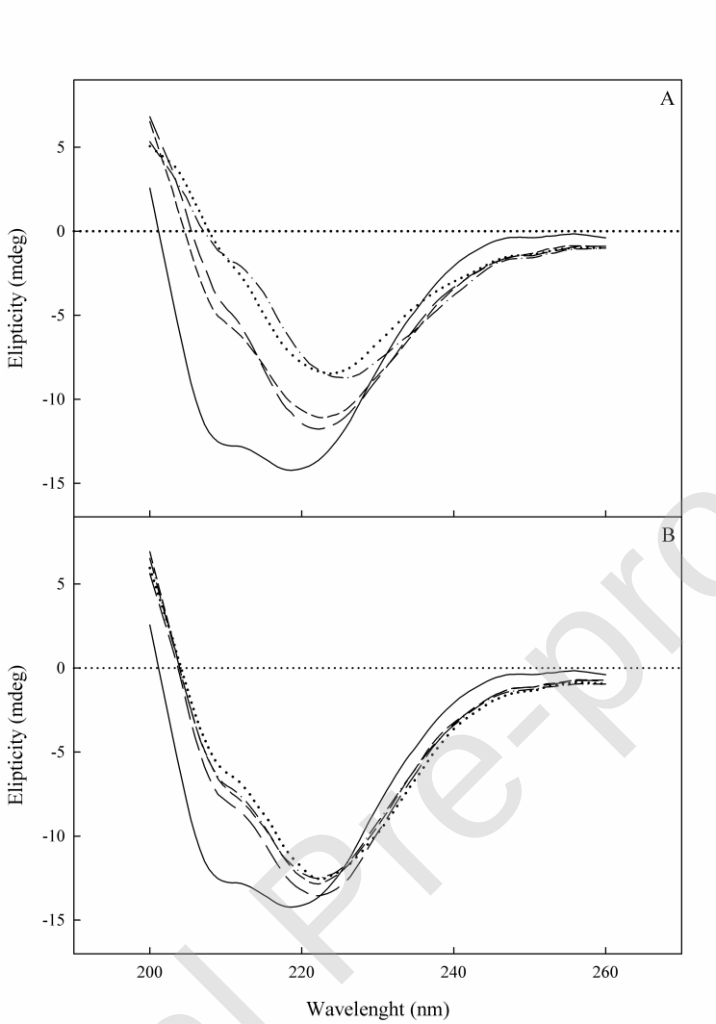

Figure 2: Far-UV circular dichroism spectra obtained at 20°C for 0.11 g/L α-Amy in the absence and in the presence of different concentrations of (A) PAA 240,000: PAA: α-Amy ratios 1:135 (——), 1:126 (---), 1:117 (—·—), 1:88 (····) and pure α-Amy (—) and (B) PAA 100,000: PAA: α-Amy ratios 1:46 (——), 1:42 (---), 1:39 (—·—), 1:25 (····) and pure α-Amy (—).Medium phosphate buffer 50 mM, pH 3.00.

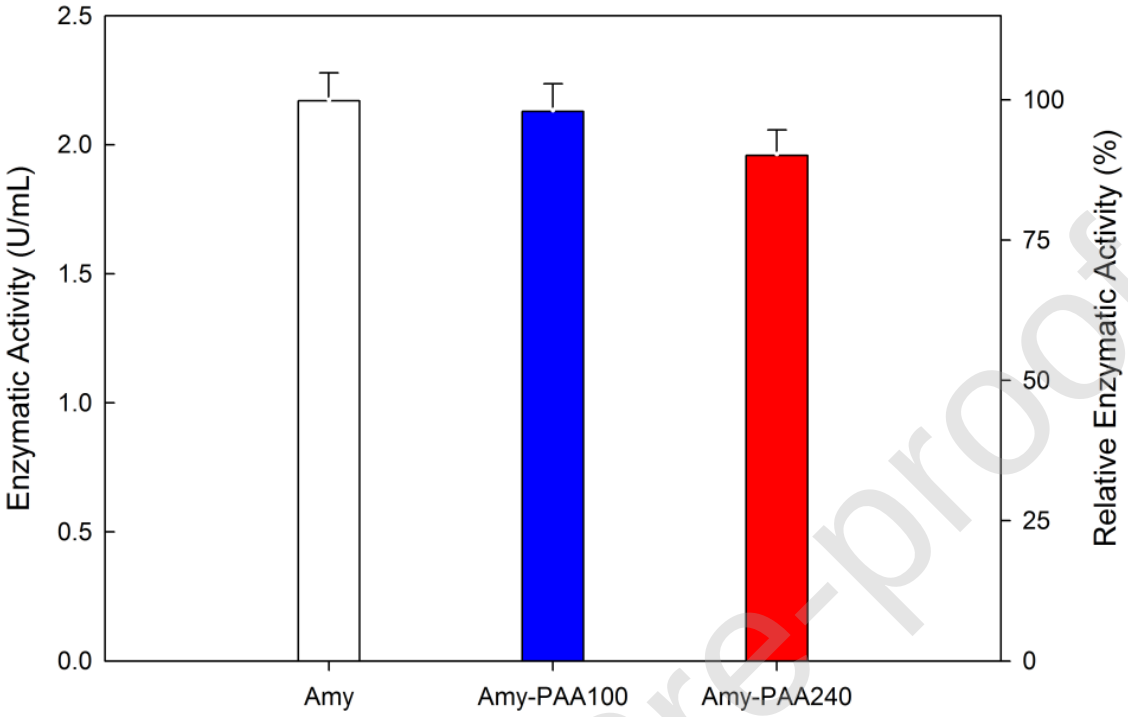

Figure 3: Enzymatic activity of α-Amy in the absence and in the presence of PAA obtained at 20°C. (□) pure α-Amy alone, 0.55 g/L. (■) PAA 100,000:α-Amy, ratio: 1:46 and (■) 240,000 :α-Amy ratio 1:135. Medium phosphate buffer 50 mM, pH 6.00.

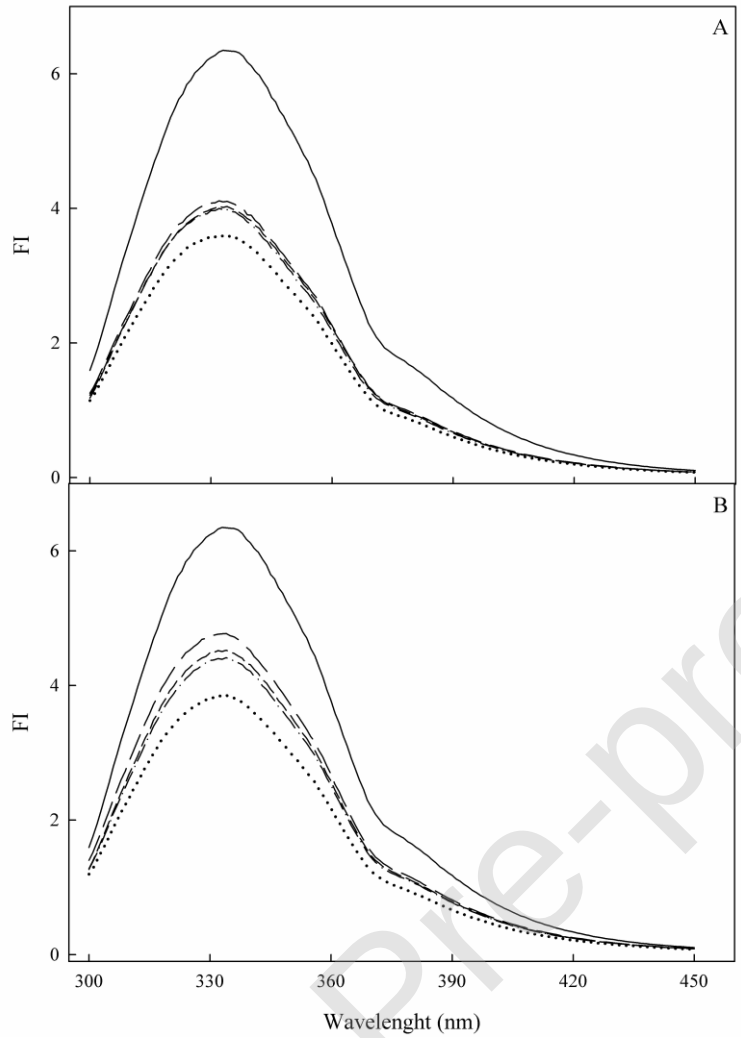

Figure 4: Fluorescence emission spectroscopy spectra obtained at 20°C for 0.55 g/L α-Amy in the absence and in the presence of different concentrations of (A) PAA 240,000: PAA: α -Amy ratios: 1:135 (——), 1:126 (---), 1:117 (—·—), 1:88 (····) and pure α-Amy (—) and (B) PAA 100,000: PAA: α -Amy ratios: 1:46 (——), 1:42 (---), 1:39 (—·—), 1:25 (····) and pure α-Amy (—). Medium phosphate buffer 50 mM, pH 3.00.

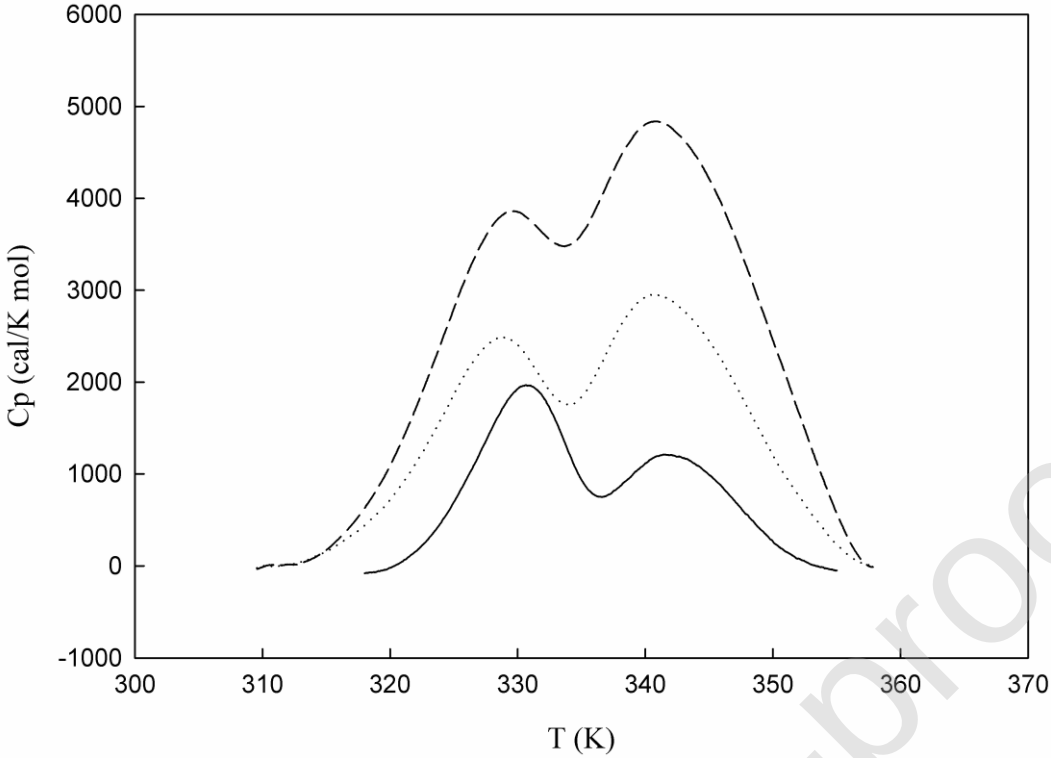

Figure 5: DSC thermogram of 22 g/L α-Amy in the absence (—) and in the presence of PAA 240,000 (⦾····) and 100,000 (——). PAA: α-Amy ratios: 1:154 (PAA 240,000) and 1:52 (PAA 100,000). Medium phosphate buffer 50 mM, pH 6.00.

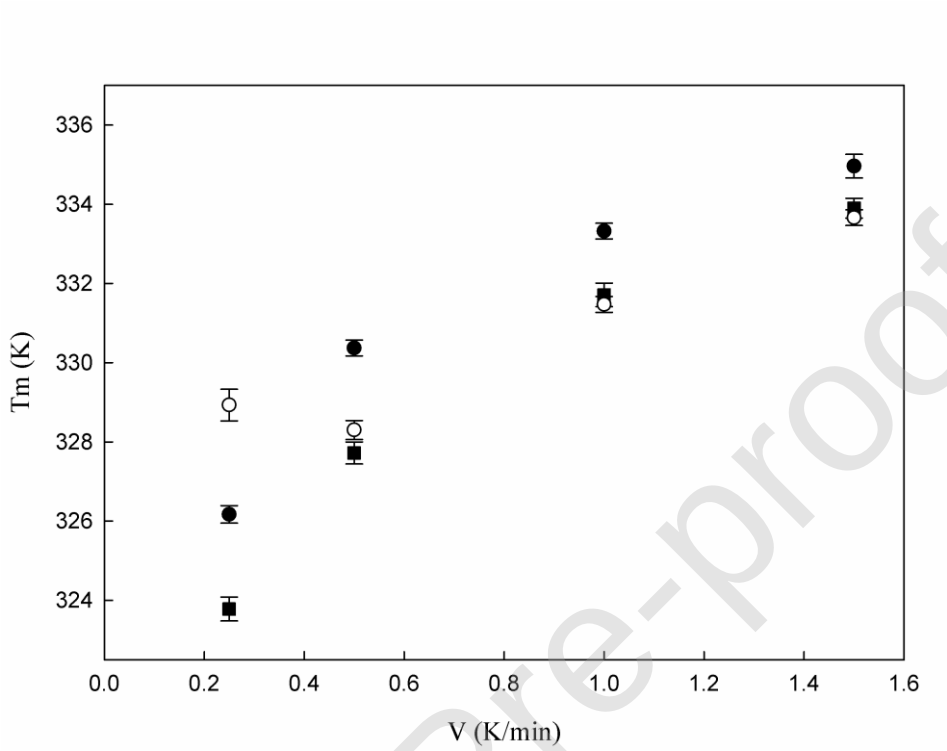

Figure 6: Dependence of Tm_1 with scan rate: α -Amy in the absence (●) and in the presence of PAA 240,000 (■) and 100,000 (○).

TABLES:

Table 1

Binding parameters between α-Amy and PAA 240,000 and 100,000, according to the single set of identical and independent binding sites model: enthalpic change (ΔH°), affinity constant (K), number of binding sites (n), free energy change (ΔG°) and entropic change (ΔS°), T= 20°C

	ΔH° (kJ/mol)	K	n	ΔG° (kJ/mol)	ΔS° (J/K mol)	[NaCl] (M)
PAA 240,000	$-7.02 \pm 1\ 10^{-2}$	$2.7\ 10^{4} \pm 2.10^{3}$	476 ± 2	$-25.02 \pm 2\ 10^{-2}$	61.5 ± 0.4	0
PAA 100,000	$-12.72 \pm 4\ 10^{-2}$	$2.1\ 10^{3} \pm 2.10^{2}$	136± 4	$-18.74 \pm 2\ 10^{-2}$	20.5 ± 0.8	0
PAA 240,000	$-3.63 \pm 2\ 10^{-2}$	$1.9\ 10^{4} \pm 3.10^{3}$	313 ± 3	$-24.14 \pm 4\ 10^{-2}$	70 ± 1	1
PAA 100,000	$-12.76 \pm 4\ 10^{-2}$	$1.9\ 10^{3} \pm 2.10^{2}$	76 ± 1	$-18.49 \pm 3\ 10^{-2}$	19.7 ± 0.4	1

Table 2

Thermal unfolding and kinetic parameters of α-Amy in the presence and in the absence of PAA

	α-Amy	α-Amy: PAA240,000	α-Amy: PAA100,000
Thermal unfolding parameters: First scanning			
Tm_1 (K)	330.37 ± 0.01	327.72 ± 0.02	328.3 ± 0.03
$\Delta H°_{cal\ 1}$(kJ/mol)	74.1 ± 0.2	115.1 ± 0.4	184.5± 0.1
Tm_2 (K)	342.73 ± 0.02	342.23 ± 0.02	342.49 ± 0.02
$\Delta H°_{cal\ 2}$ (kJ/mol)	52.3 ± 0.2	177.8 ± 0.4	322.6 ± 0.1
Thermal unfolding parameters: Second scanning			
Tm_1 (K)	334.3 ± 0.1	-	-
$\Delta H°_{cal\ 1}$(kJ/mol)	27.6 ± 0.8	-	-
Tm_2 (K)	342.69 ± 0.05	340.34 ± 0.02	339.35 ± 0.02
$\Delta H°_{cal\ 2}$ (kJ/mol)	514.6 ± 0.8	127.6 ± 0.4	266.9 ± 0.4
Kinetic parameters			
$E^{\#}$ (kJ/mol)	221 ± 4	238 ± 12	213 ± 12
T* (K)	339.6 ± 0.6	338 ± 1	338 ± 1